Magnetic dichroism in Co films on Cu(001) using unpolarized light: A thickness and temperature dependent study

Xingyu Gao, M. Salvietti, W. Kuch, C. M. Schneider, [1] and J. Kirschner

Max-Planck-Institut für Mikrostrukturphysik, Weinberg 2, D-06120 Halle, Germany

Abstract

The thickness and temperature dependence of the angular distribution of the magnetic dichroism in photoemission from Co 2p core levels of Co/Cu(001) ultrathin films has been investigated, using unpolarized Mg K_α radiation. Photoelectron spectra were collected for emission angles in a range of $\pm 9^\circ$ around the surface normal in the [001] azimuth. All asymmetry spectra were found to exhibit an identical spectral shape within the experimental error bar, but different scaling. The angular distribution of the Co 2p dichroic signal shows that at emission directions off the sample normal strong variations are present, in contrast to predictions from simple atomic theory. These crystallinity-related modulations were studied for Co films of different thicknesses (5, 3, 2, and 1.5 atomic monolayers (ML)) and different temperatures (100 and 300 K). They are higher for thicker films and lower temperatures. This experimental finding proves a diffraction picture, in which this modulation around the surface normal is explained by diffraction effects in forward scattering along the sample normal. As diffraction effects in magnetic dichroism combine both diffraction and magnetic dichroism, its behavior is influenced by both, structural and magnetic properties of the film.

Keywords: Magnetic dichroism; Photoelectron spectroscopy; Photoelectron diffraction; Magnetic thin films

[1] present address: Institut für Festkörper- und Werkstoffforschung, Postfach 27 00 16, D-01171 Dresden, Germany

1 Introduction

Core level photoelectron spectroscopy is a useful technique to study, on an element resolved basis, the electronic structure of solids. In particular, when applied to magnetic systems, it permits one to observe magnetic interactions between the spin polarized and exchange split valence electrons and the core hole formed during the photoemission process [1–6]. The photoemission line splitting caused by these interactions is normally very small compared to the width of the core level photoemission line so that it can be detected only using spin resolved photoemission [7–9]. Magnetic dichroism in x-ray photoemission has been introduced as an alternative to this technique [10]. In magnetic dichroism experiments one measures the changes in the core level spectra upon changing the relative orientation of light polarization and magnetization. This kind of dichroism appears in angle-resolved experiments and is usually named magnetic dichroism in angular distribution (MDAD). The first experiments performed with this technique used circularly polarized light [10–13]. Later on, similar effects have been observed using linearly polarized light [14–16], and unpolarized radiation [17–20].

In MDAD using linearly polarized light (LMDAD) the dichroism is a pure interference effect, arising from the interference of different components of the dipole operator [13,16,21]. From another point of view it can thus be regarded as being proportional to the product between the reduced dipole matrix elements $t_s t_d$, where each term corresponds to the allowed transitions $p \rightarrow s$ and $p \rightarrow d$ [15]. The dichroism is observable only if the magnetization $\mathbf{M}$ has a component perpendicular to the plane defined by the photon and photoelectron wavevectors, and if this $\mathbf{M}$-component is not aligned with the photon polarization. This means that s-polarized light thus does not give any contribution to the dichroism [21,22].

As unpolarized light can be considered an incoherent superposition of s-polarized light and p-polarized light, magnetic dichroism using unpolarized radiation is basically equivalent to the dichroism observed using linearly p-polarized light, apart from a constant scale factor. This permits one to perform experiments of magnetic dichroism with unpolarized light using a conventional x-ray source.

The theoretical explanation of LMDAD relies upon the well known effects of spin polarization of photoelectrons excited from a beam of polarized atoms and molecules [23,24]. In other words, these effects can to first order be interpreted as a solid state manifestation of the linear dichroism in the angular distribution (LDAD) of photoelectrons in atomic photoionization, where the exchange interaction between valence and core states polarizes the core hole [24,25]. The first reports on LMDAD proposed a phenomenological explana-

tion of the effect in connection with experimental results on atoms of rare gas [26], and with atomic theory [15,27].

The photoionization of a closed subshell, in the situation when the final hole is polarized, is equivalent to the photoionization of a one-electron subshell, which is initially polarized [22,28]. For that reason LMDAD from ferromagnets could be treated like photoemission from initially polarized atoms, provided that the splitting of the hole state due to the exchange interaction with the $3d$ subshell is taken into account (atomic-like dichroism). Cherepkov pointed out that the applicability of the atomic model requires photoelectron kinetic energies high enough (at least at energies $\geq$40 eV) to ensure that the interaction of the emitted electron with the remaining electronic system of the solid can be considered negligible. It is therefore possible to simplify the final state problem, and to discuss the one hole spectrum of the $2p$ core level only. In that description no crystallinity effects are included.

In particular, using equation (1) of Cherepkov's theory (Ref. [22]), in an experimental geometry where the sample magnetization $\mathbf{M}$ is switched between up and down, being perpendicular to the plane defined by the photon and photoelectron wavevectors ($\mathbf{q}$ and $\mathbf{k}$, respectively), the dichroic asymmetry in LMDAD (defined as the photoemission intensity difference of the two magnetization directions, $\mathrm{I}(\mathbf{M}) - \mathrm{I}(-\mathbf{M})$) can be written as

$$I^{LMDAD} = I(\mathbf{M}) - I(-\mathbf{M}) \propto \rho^n_{10} C^j_{221} (\mathbf{k}\cdot\mathbf{q})(\mathbf{q}\cdot\mathbf{k}\times\mathbf{M}) \tag{1}$$

where the parameter C^j_{221} is

$$C^j_{221} \propto \sin(\delta_2 - \delta_0). \tag{2}$$

Here δ_0 and δ_2 are the corresponding phase shifts of the reduced dipole matrix elements for the $p \rightarrow s$ and $p \rightarrow d$ transitions, respectively. As it appears from equation (1), the sign and the relative magnitude of LMDAD, for different magnetic sublevels, are defined exclusively by the sign and the magnitude of the state multipoles ρ^n_{10}, which define the orientation of the hole state.

This description of the atomic-like dichroism does not include any effects of the crystallinity, represented by the surface normal $\mathbf{n}$. In an experimental geometry in which the sample is rotated about the magnetization axis, and the direction of the three vectors $\mathbf{q}$, $\mathbf{k}$, and $\mathbf{M}$ is kept constant, the atomic-like dichroism is independent of the emission angle α, defined as the angle between the sample normal $\mathbf{n}$ and the photoelectron wavevector $\mathbf{k}$ (cf. Eq. (1)).

However, when an angle-resolved photoemission experiment on solids is performed, other effects, which modify the atomic-like dichroism, can be important. In particular, recent MDAD experiments have shown that a strong

modulation of the angular distribution of the atomic-like dichroism appears [18,29–31]. In those experiments it was observed that crystallinity effects were present for emission directions off the sample normal, giving rise to a characteristic checkerboard pattern in the combined angle and energy dependence of the dichroic asymmetry. Such strong effects are also present around other low index directions [18,30,31], whereas along these directions the dichroism was found to be mainly of atomic character [18,30].

These crystallinity effects have been interpreted as an additional diffraction contribution to the atomic-like dichroism [18,29–31]. The theory of photoelectron diffraction [32–35] in fact predicts that the scattered waves at the detector will have acquired a phase shift with respect to the direct wave, due to the scattering processes and the difference in path length of the waves. The amplitude and the phase shift of the scattered waves depend on the emission angle α, the spin of the photoelectron, and the magnetic moment of the scatterer atom. In consequence, the total amplitude at the detector, composed by amplitudes of the direct and scattered waves, will be a function of α [18]. From that it follows that the dichroic asymmetry is a function of the emission angle [18,30].

The purpose of the present investigation is to test this diffraction picture. We performed a thickness (5, 3, 2, and 1.5 atomic monolayers (ML)) and temperature (100 and 300 K) dependent study of angle resolved magnetic dichroism of Co/Cu(001) films, using unpolarized light. A possible diffraction contribution at the photoelectron energies between 450 and 550 eV (the energy range exploited in this study) should be mainly governed by forward scattering effects [32–35]. For that reason, when decreasing the film thickness the diffraction is expected to show a strongly reduced influence on the dichroism, due to the lack of atoms available for forward scattering. From photoelectron diffraction theory it is well known that the diffraction effects in photoemission are also influenced by thermal vibrations of the atoms in the solid, which affect the scattering coherence in otherwise periodic structures, and thus reduce the photoelectron intensity and broaden its angular distribution [32–35]. This should be reflected, at constant film thickness, in a dependence of the diffraction effect on the film temperature, where for higher temperatures a smaller effect is expected.

Co/Cu(001) is a good candidate for this investigation because of the well-known epitaxial layer-by-layer growth and its well-known magnetic [36–43] and structural properties [37,44–49]. Moreover, recent experiments have shown that using LMDAD it is possible to obtain information on the spin dependent electronic correlations present in photoemission spectra of 3*d* ferromagnetic metals [19]. In particular, Schneider *et al.* have shown by an MDAD experiment that for 5 ML Co/Cu(001) films there is evidence in the Co 2*p* photoemission line for a many-body satellite with majority spin character, which

appears as a negative peak in the dichroic asymmetry [19]. For that reason, knowing the shape of the dichroic signal for films at different Co thicknesses should help to understand the electronic structure of the ground state of this element.

2 Experiment

The experiment was performed using a standard Mg K_α x-ray source emitting unpolarized light at 1253.6 eV, and a commercial multichannel hemispherical electron energy analyzer (HA 150 VSW Scientific Instruments Ltd.). The energy resolution of the spectrometer was set to 320 meV, and the overall resolution, including the width of the photon energy line, was about 0.9 eV. The photoelectron current measured on the sample, at typical working conditions of the x-ray source, was ~ 3 nA. The angular resolution of the electron detection was better than $\sim 3^\circ$, and the angular reproducibility of the sample manipulation $\sim 0.2^\circ$.

The samples were thin Co films grown on Cu(001). Prior to the film preparation the copper substrate was cleaned by 1.5 keV Ar^+ ion bombardment and annealing cycles to about 800 K for 2 min and to 600 K for 5 min. The cleanliness of the substrate was monitored in situ by Auger electron spectroscopy (AES). The growth was epitaxial, and proceeded layer-by-layer. Cobalt films were deposited in situ on Cu(001) at room temperature by electron bombardment of a high purity cobalt rod (99.99%) with a typical deposition rate of 1 ML/min. Before deposition, a proper outgassing of the Co rod had been performed. In this way the pressure in the chamber remained in the range of 10^{-8} Pa during deposition, and no impurities could be detected by Auger electron spectroscopy. Film thickness and growth conditions were monitored by medium energy electron diffraction (MEED), following the intensity variation of the specular electron beam during evaporation. The growth temperature was carefully controlled by cooling the sample with liquid nitrogen and heating to the desired temperature, which was stabilized within a range of $\pm$ 5 K. The thickness of all of the films studied in this investigation is defined within a range of ± 0.2 ML.

The magnetic properties of the films were studied by in-situ magneto optical Kerr effect (MOKE). Earlier studies showed that there is a pronounced in-plane four-fold anisotropy, which was suggested to be due to a strain-induced magnetoelastic anisotropy [37–41]. In the present experiments, it was found that higher magnetic fields are needed to fully magnetize the Co films along the <100> hard axis than along the <110> easy axis. The remanent magnetization along all in-plane directions, however, was found to be equal to the saturation magnetization (within our level of accuracy), allowing to study

these films with MDAD along both directions.

Before recording each photoelectron spectrum, the sample was remanently magnetized in-plane along the [010] direction of the substrate by applying a magnetic field obtained by a current pulse through a magnetic coil located near the sample. The current pulse is supplied by discharging a capacitor of 4 mF into the coil with the axis along the [010] direction of the sample. To check the sample magnetization, MOKE measurements were performed between and after the photoemission measurements with reversed magnetization. It was found that the sample was remanently magnetized in saturation during all the time needed for each measurement, for all the Co films investigated in this paper.

We have collected the photoemission intensity spectra (I^+ and I^-, respectively), for the two magnetization directions, as defined in Fig. 1. All the intensity spectra reported in this paper have been collected with the same conditions of the x-ray source (emission current 40 mA and anode high voltage 15 kV), except those of the 5 ML film at 300 K, which have been measured accidentally with a lower emission current (35 mA).

From these curves we have formed the asymmetry, which is defined as

$$A(E) = \frac{I^+(E) - I^-(E)}{I^+(E) + I^-(E)}, \tag{3}$$

where E is the electron kinetic energy. The intensity at the low binding energy side of the Co $2p_{3/2}$ line has been subtracted as a constant background. The asymmetry curve is obtained after scaling I^- in order to coincide with I^+ in the higher binding energy side of the $2p$ levels, where no dichroism is expected [29].

Intensity spectra were collected in the kinetic energy range between 440 and 485 eV. The spectra presented in this paper are reproduced with a binding energy scale relative to the energy position of the Co $2p_{3/2}$ peak in the intensity spectra (778 eV binding energy), fixed as zero of the energy scale. To form the dichroic asymmetry curves shown in this paper, we have collected three times the sequence of spectra I^+ and I^-. Each intensity spectrum (I^+ or I^-) is counted for $\sim$ 3 min, giving a total counting time, in order to form an asymmetry curve, of $\sim$18 min.

In the experiments, the intensity of the x-ray radiation was found to change, especially in the first few hours after starting the source [50]. As in each intensity scan the spectrum is measured from lower to higher kinetic energies, the time-dependent variation of the intensity and some other changes of the experimental situation during the measurement can cause the baseline of the

asymmetry spectrum to be tilted, which cannot be corrected just by simply rescaling. Because the goal is to study the small effects in the angular dependence of the magnetic dichroism, it is crucial to have a reliable criterion to fix the baseline of the dichroic asymmetry spectra. As the time needed for the acquisition of one dichroism spectrum is short compared to the time constant of the experimental decay of the x-ray intensity [50], the baseline can be assumed to have a linear slope. In all the reported MLDAD experiments of Co films in this paper, the shape of the asymmetry spectra of the $2p$ levels is very similar (this will be demonstrated later). Performing a more systematic data analysis to overcome tilted baselines, a template asymmetry spectrum $template(E)$ was used to fit every asymmetry spectrum $Asy(E)$. This procedure will be called "template fit" in the following. The idea is to minimize the chi-square:

$$\chi^2 = \sum_i ((Asy(E_i) - c_0 \cdot template(E_i) - c_1 - c_2 E_i)/\sigma_i)^2 \tag{4}$$

by variation of the parameters c_0, c_1, and c_2. Here i is the index for the data points, E_i is the respective relative binding energy of data point i in this asymmetry spectrum, and σ_i is the standard deviation for each data point from Poisson statistics, correlated to the count rate N_i by $\sigma_i = 1/\sqrt{N_i}$. The parameter c_0 is the scaling factor for the dichroic asymmetry spectrum with respect to the template spectrum, c_1 a constant offset of the baseline, and c_2 corresponds to the slope of the tilted baseline. In this way, the baseline shape can be systematically adjusted by the parameters c_1 and c_2 to the baseline of the template curve. The corrected data points can then be obtained from the results of $Asy(E_i) - c_1 - c_2 E_i$. For the present data, c_1 was always below 1%, and c_2 between 0 and 0.04%/eV. The values of these two parameters depend mainly on the stability of the x-ray light intensity. As the parameter c_0 describes the relative size of the magnetic dichroism, it can be used to study the angular dependence of the magnetic dichroism for all spectra. As template asymmetry curve the spectrum of a 10 ML Co film, which has a good signal-to-noise ratio, was used in this paper. As result for the size of the asymmetry the parameter c_0 times the peak-to-peak asymmetry of the template curve is presented. For this procedure it is assumed that the spectral shape of the asymmetry curves does not vary. We will show in the following section that this is indeed the case.

In our experimental geometry (Fig. 1), the angle between the photon and photoelectron wavevectors is fixed at 45^0. Angular distribution spectra are collected after a rotation of the sample around the direction of magnetization, and presented as a function of the angle α, which is the angle between the photoelectron emission wavevector and the surface normal ($\mathbf{k}$ and $\mathbf{n}$, respectively). In that way the relative orientation of the vectors $\mathbf{k}$, $\mathbf{q}$ and $\mathbf{M}$ is fixed, and only the photoemission direction and the light incidence direction with

respect to the crystal lattice are varied (see Fig. 1).

3 Results

In Fig. 2 (a) Co $2p$ intensity spectra for the two opposite directions of magnetization for 5 ML Co/Cu(001) are reported. These spectra have been collected at an emission angle $\alpha = 0$, and at a sample temperature of 100 K. They show the two spin-orbit split $2p$ levels, $j{=}\frac{3}{2}$ and $j{=}\frac{1}{2}$, separated by $\sim$15 eV. A broad structure centered at $\sim$4 eV (marked in Fig. 2 (a) with an arrow) is also clearly visible. It presents higher intensity for magnetization down (down triangles). The spectra reported here agree qualitatively well in terms of lineshape and energetic position of the Co $2p$ lines with others obtained earlier at the same Co thickness [19]. The $2p$ intensity lineshapes appear slightly asymmetric, with the higher binding energy side of the lines enlarged, in good agreement with the Doniach-Šunjić-type lineshape [51].

In Fig. 2 (b) the asymmetry function is depicted after the template fit baseline correction. The data points (open circles) are corrected with a line slope $-0.0068 + 0.00019E_i$, as explained in Sec. II. The solid line is the scaled template asymmetry spectrum. It is obvious that the template fits the spectrum well within the experimental error bars. The asymmetry presents the typical "plus/minus" features of the $2p$ lines [10,19,29]. In the case of the $2p_{3/2}$ level, the "plus" feature is clearly visible at about -1.1 eV (A in Fig. 2 (b)), while the "minus" feature appears as a shoulder at about 1.5 eV (B in Fig. 2 (b)) on a wide negative structure. For the $2p_{1/2}$ state the situation is reversed with the "minus" feature centered at $\sim$ 14 eV and the "plus" feature at $\sim$ 17 eV. The region in between the two states is negative with a superimposed feature at $\sim$ 4 eV (C in Fig. 2 (b)), which reflects the difference in emission intensity for the two magnetizations in this energy region (cf. Fig. 2 (a)). In analogy with previous magnetic dichroism investigations using linearly polarized light [15,29] and unpolarized light [19], we attribute the dichroic feature centered at -1.1 eV as due to the intensity difference for emission mainly from the $\mathrm{m}_j = \pm 3/2$ projections of the Co $2p_{3/2}$ core level.

In Fig. 3 a series of dichroic asymmetry spectra for 5 ML Co/Cu(001) at 100 K after baseline correction over an emission angle range from $\alpha = -9°$ to $\alpha = +7.5°$ is shown. The symbols represent the measured data points after baseline correction, the solid lines are the template spectrum scaled with a different factor c_0 for each angle. It is obvious that the template curve fits all the spectra well within the experimental error bars. An energy shift of "plus/minus" and "minus/plus" features related to the $j = 1/2$ and $j = 3/2$ levels as a function of α, as it was observed in Ref. [18], cannot be confirmed from the present data within the spectral resolution. Fig. 3 shows that the size

of the asymmetry varies strongly even when the emission angle is changed by a very small amount about the surface normal direction ($\alpha = 0$). The asymmetry even changes its sign at $\alpha = +3°$.

Fig. 4 shows the dichroic asymmetry curves for 5 ML Co/Cu(001) at T = 300 K at the same emission angles. It is clear that the template asymmetry spectrum again fits well every spectrum. The 300 K data exhibit a similar but smaller variation of the asymmetry with the emission angle α as in the case for $T = 100$ K.

In Fig. 5 (a) we show the angular distribution of the total intensity of the Co $2p_{3/2}$ peak, obtained by summing up the $2p$ intensity spectra for the two opposite magnetizations ($I^+ + I^-$), for 1.5, 2, 3, and 5 ML Co film thickness at 100 K. The angular distribution shows a clear peak located at $\alpha = 0$ for the 5 ML and 3 ML films, while for 1.5 and 2 ML only weak indications of a maximum along the sample normal are present. This shows that strong focusing effects along the sample normal due to photoelectron diffraction are present for the 5 ML and 3 ML films. These effects appear to be strongly reduced for the 2 and 1.5 ML films. Fig. 5 (b) summarizes the angle dependence of the peak-to-peak asymmetry. Shown is the parameter c_0 in units of the peak-to-peak asymmetry of the template curve as a function of the emission angle α at various thicknesses (5, 3, 2, and 1.5 ML). The markers represent the measurements. The lines are for guiding the eye. The angular distribution of the experimental points corresponding to the 5 and 3 ML films exhibits an angular modulation with an approximately sinusoidal shape. For the 2 and 1.5 ML films, even if less visible, this sinusoidal modulation is still present. Fig. 5 (b) shows clearly that the amplitude of the modulation is reduced with decreasing film thickness.

In Fig. 6 (a) we present the angular distribution of the total intensity of the Co $2p_{3/2}$ peak ($I^+ + I^-$) for the 5 ML film measured at 100 K and 300 K. The angular distribution of the 300 K measurement has still a peak located at $\alpha = 0$. However, it is much broader, and the peak at $\alpha = 0$ is much less prominent compared with the curve measured at 100 K for the same thickness, even considering the lower photoemission intensity for this film at all emission angles due to the 12.5% lower light intensity used (as mentioned in Sec. II), which was not corrected in Fig. 6 (a). Fig. 6 (b) shows the corresponding parameter c_0 in units of the peak-to-peak asymmetry of the template curve as a function of the emission angle for 5 ML at 100 and 300 K, respectively. It is clear that the amplitude of the modulation is reduced at 300 K with respect to that at 100 K.

4 Discussion

Figs. 5 (b) and 6 (b) show clearly that the dichroism of 5 ML and 3 ML Co films varies strongly around the sample normal. The 2 ML and 1.5 ML films present less angular dependence of the dichroic signal, but nevertheless there are still small modulations. This is surely a deviation from the atomic description of the dichroism, as discussed in the introduction. This deviation then must be attributed to the crystallinity of the sample, which is not included in atomic models. In the following we will show that the modulation of the dichroism of the Co films can be mainly interpreted as an additional diffraction contribution to the atomic-like dichroism. Besides, the crystallinity of the sample may manifest itself also in effects not related to photoelectron scattering. The atomic model, described in the introduction, is valid only for an isolated atom that is polarized along **M**, but has an otherwise spherically symmetric electronic configuration. This is surely not a valid description for atoms in a solid. There the atoms and their electronic orbitals are kept fixed in space. In addition, a directional redistribution of the electronic states compared to free atoms due to the presence of neighboring atoms may occur. In such a case the photoelectron will probe a non-spherical potential, and as a consequence the outgoing electron wave (direct wave) could present a small angular dependence [52]. By varying the emission angle in our experimental geometry, we change the direction of light incidence on the sample. The excitation process depends on the angle of incidence. In particular we have to recall that LMDAD for the atomic model involves a phase shift difference $\delta = \delta_2 - \delta_0$ between the two interfering final state channels with $l = 0$ and $l = 2$ angular momentum (s and d waves), considering the transitions allowed by the dipole interaction, whereby the dichroism scales with $\sin\delta$. As the emission angle and incidence angle are changed, the matrix element for the excitation will change, and consequently also this phase shift. However, as the core-level electrons are very localized, and the kinetic energies for the outgoing photoelectrons are larger than 400 eV in the present experiments, this effect is expected to be smaller than diffraction effects.

Photoelectron diffraction in MDAD arises from the interference between the scattered waves scattered by nearby atoms and the direct wave, as discussed in the introduction. As the forward scattering dominates in the diffraction at the present kinetic energies [32–34,53], it will be the main contribution to the diffraction effects. For a more quantitative analysis of the present data, we will now discuss the angular distribution of the dichroic signal reported in Figs. 5 (b) and 6 (b) together with the one calculated using a simple heuristic diatomic single-scattering model. That model has been introduced by Fanelsa *et al.* [18], and later refined by Schellenberg *et al.* [19], to describe an MDAD experiment using unpolarized light in a geometry equivalent to the one used in the present investigation.

That model predicts that in forward scattering conditions (small emission angles) the diffraction contribution to the dichroic asymmetry $A(\alpha)$ for off-normal emission is dominated by the following term

$$A(\alpha) \propto \mid f(\alpha) \mid \sin[\delta(\alpha)]\alpha, \tag{5}$$

where $\delta(\alpha)$ and $f(\alpha)$ give the phase shift and the scattering amplitude of the process, respectively. As discussed in Ref.[32–34], $\delta(\alpha)$ and $f(\alpha)$ are both non-zero and slowly varying with α near forward scattering, so that equation (5) gives a dichroic asymmetry which is antisymmetric around 0. Along the sample normal the dichroism was found to be mainly free atom-like [19]. Considering the photoemission process equivalent for opposite angles with respect to 0° is a good approximation for small values of the angle α, as far as we can neglect the effects due to the variation of the light incidence. From Figs. 5 (b) and 6 (b), it is seen that the dichroism exhibits an antisymmetric angular behavior with respect to a point on the $\alpha = 0$ ordinate. Therefore, our results partially prove the simple diffraction picture.

To further test the diffraction picture in MDAD, we can discuss the thickness dependence of MDAD. For each position in a 5 ML Co film, theoretically, there are 1 or 2 Co atoms that scatter along the [001] direction of an fcc film, compared to only 0 or 1 atom for 3 ML Co films, and no atom for 2 and 1.5 ML Co films. Therefore, the intensity peaks at normal emission should be reduced with decreasing thickness, as was proven from Fig. 5 (a). As forward scattering dominates the diffraction effects, the variation of dichroism due to diffraction should be consequently reduced. This is represented in Fig. 5 (b) by the decrease and broadening of the modulation in passing from thicker to thinner films. In particular for 1.5 ML the modulation becomes strongly reduced and broad, but is still present. For an ideal layer-by-layer grown 1.5 ML film, this can not be understood from a simple forward scattering picture.

To clarify the origin of the modulation at 2 and 1.5 ML (cf. Fig. 5 (b)), we must consider the structure of these films with thicknesses of less than 3 ML. Many studies are present in literature on the growth of Co on Cu(001) [37,47,44–46,48]. At small thicknesses (less than 2 ML), the Co films are found to be composed by a significant amount of bilayer islands resulting in a strong deviation from the ideal layer-by-layer growth [37,48]. Starting from 2 ML, the growth mode changes and becomes more perfect layer-by-layer, but the film still contains a certain number of voids and additional islands [37,48]. The roughness at integral coverages is found to be confined to the uppermost layer, and to be of the order of ± 1 ML [37]. Third layer islands could thus contribute to forward scattering events in normal emission in 2 ML film, but not for 1.5 ML, where no 3 ML height islands were found [48]. It was also reported [48,49] that a small amount of Co atoms is intermixing with substrate atoms in the submonolayer range (for 1 ML about 0.25 ML Co atoms [48]). There was a

hint that these Co atoms embedded in the Cu surface act as pinning sites and lead to heterogeneous nucleation of additional Co islands [48,49]. Intermixing Co atoms in 1.5 ML and 2 ML Co films, therefore, would also have forward scatterers along the sample normal. This would explain the small peaks along the sample normal in the intensity distribution of these Co films in Fig. 5 (a). In this way, the small modulations for the 2 ML and 1.5 ML films could be explained in the forward scattering picture.

Of course, other effects related to the crystallinity of the sample as discussed before may also contribute to the residual modulations at 1.5 ML and 2 ML Co thickness. Moreover, as discussed in Refs. [32–35] and [53], at photoelectron kinetic energies between 450–550 eV small effects due to non-forward scattering could still influence the dichroic signal. Although all these effects could be partially responsible for the angular distribution in the 1.5 ML and 2 ML Co films, we believe that they are mostly influenced by the forward scattering from Co atoms embedded in the Cu substrate, as the small peaks along the sample normal in the intensity distribution of 1.5 film are a hint for forward scattering along this direction. The diffraction effects in the magnetic dichroism are only related to the magnetic atoms, so that we can conclude that these Co atoms embedded in the Cu substrate must be ferromagnetic, but may have a reduced magnetic moment. This shows the power of forward scattering as a method for a surface sensitive study in the monolayer range.

As discussed in the introduction, the film temperature affects the photoelectron diffraction effects through the Debye-Waller factor [32–35]. In particular a loss of constructive interference between the undiffracted and diffracted photoelectron waves is expected for higher temperatures, that should be reflected in a reduction of coherent scattering effects and a broadening of the angular distribution of the intensity, and of the asymmetry. This is in good agreement with the observed broadening of the intensity angular distribution (Fig. 6 (a)), and with the decrease and broadening of the modulation observed in MDAD passing from 100 K to 300 K sample temperature (see Fig. 6 (b)). This generally proves the diffraction picture in MDAD and shows that the crystallinity effects in the 5 ML Co film are mainly diffraction effects, as other crystallinity effects are less influenced by the temperature.

In order to compare the size of the dichroism at different thicknesses and temperatures, it is very important to separate the apparent crystallinity effects (mainly from forward scattering) from the "atomic" dichroism. Of course, there is no real atomic dichroism in a solid, as each photoemission intensity spectrum reveals already the electronic structure of the solid. However, we can still use the word "atomic" to describe the dichroism which is related to the direct wave, in order to distinguish it from the modulation by diffraction effects. As was shown above, all the measured asymmetry spectra could be fitted well by the template curve within the error bars. This proves that diffraction

effects do not create a new dichroism, but superimpose a modulation to the "atomic" dichroism (atomic-like dichroism).

As discussed above, for emission along the sample normal, the atomic-like dichroism should dominate [18,30]. Taking thus the dichroism at $\alpha = 0$ as the atomic-like dichroism, it is seen from Fig. 5 that it is reduced for decreasing the film thickness. For example, the dichroic asymmetry at the sample normal for 1.5 ML is $(45 \pm 14)\%$ of the dichroic asymmetry for 5 ML, $(2.0 \pm 0.5)\%$ and $(4.4 \pm 0.3)\%$, respectively. Recently Schellenberg *et al.* [30] performed an LMDAD experiment using unpolarized light in an Fe-based amorphous sample ($Fe_{78}Si_{13}B_9$ metallic glass). They found that the atomic-like dichroism of Fe is reduced in the metglass sample (70%) with respect to epitaxial Fe films, and that this reduction is mostly due to the smaller Fe magnetic moment in the metglass (86%). Within this picture the different value of the asymmetry for the two thicknesses could be partially explained considering a smaller magnetization in the 1.5 ML film. The Curie temperature of a 1.5 ML film is just 130 K [37], which is very close to the temperature of the measurements (100 K), so the remanent magnetization could be smaller by about 20% [54] compared with that at 0 K. For 5 ML T_c is far above room temperature (850 K [37]), so the difference between 0 and 100 K is negligible. If we assume the average magnetizations of both films at 0 K to be the same, the smaller average magnetization of the 1.5 ML film at 100 K could be one reason for the reduction of the "atomic" dichroism at 1.5 ML.

Also other mechanisms could be responsible for a smaller "atomic" dichroism at 1.5 ML. Here we recall that LMDAD involves a phase shift $\delta = \delta_2 - \delta_0$ between the two interfering final states with $l = 0$ and $l = 2$ (cf. Sec. I). There is no reason that this phase shift has to be identical for Co atoms in 5 and 1.5 ML films. A different phase shift could modify the atomic-like dichroism differently in the two films, and could be one reason for the different "atomic" dichroism at these two films. It was shown also in Ref. [19] that there are small residual diffraction effects due to combined $s-$ and $d-$channel interference along the normal in the simple forward scattering picture. These residual effects can be very different for films with different thickness and for different temperatures, as forward scattering has a strong thickness- and temperature-dependence. Moreover, other crystallinity effects connected to non-forward scattering can be present along the sample normal, and different for different thicknesses and temperatures. These effects could also contribute to the decrease of the dichroism at the sample normal for the 1.5 ML film.

Let us now consider the influence of temperature on the atomic-like dichroism of 5 ML Co. The atomic-like dichroism should be affected, at a fixed film thickness, by variation of the temperature, if this results in a variation of the magnetization. However, since T_c of the 5 ML Co film is far above room temperature, the change of the average magnetization of such a film at the

measured temperatures of 100 K and 300 K is negligible. This is reflected in the experimental results, which show almost no reduction of the atomic-like dichroism within the error bars at a sample temperature of 300 K with respect to 100 K (cf. Fig. 6 (b)).

Finally we can discuss the shape of the atomic-like dichroism, which was found to be independent from thickness and temperature. As was shown in Fig. 2 (b), there is a feature centered at $\sim$ 3 eV (labeled C in the figure) superimposed on a non-zero dichroic background in the region between the $2p_{3/2}$ and $2p_{1/2}$ lines, where no dichroism is expected [29]. In Fig. 2 (a) a feature in the intensity spectra appears at $\sim$4 eV. A similar feature appears also in Fe $2p$ photoemission curves in experiments with monochromatized light [29]. For this reason it can not be due to spurious photons with higher energy, created in the x-ray source. As discussed in Ref.[19], a similar feature in energy position and lineshape has been attributed to a reminiscence of the localized nature of the d electrons of cobalt, and arises due to the interaction of the valence states with the core hole formed in the photoemission process (screening), which leads to discrete satellites in the intensity photoemission spectra. A typical example of this kind of satellite is the "6 eV" satellite of the Ni $2p$ spectrum [55,56]. A narrow d band in Ni is responsible for the formation of correlation-induced spectral features. In a similar context the feature in the Co $2p$ spectrum may be discussed. For Ni, Co, and Fe the satellites are spin-polarized and carry information about spin dependent correlations and screening processes. The spin polarization of the many body satellites gives rise to the characteristic features in the magnetic dichroism [19]. An indication of this feature is also found in the LMDAD spectrum, calculated by Thole and van der Laan [57]. Obviously for a better understanding of the influence of many body interactions on the magnetic dichroism, spin resolved photoemission from valence bands and core levels together with more detailed calculations for the electronic ground state of Co would help significantly.

5 Summary and conclusions

In this paper we have reported a thickness and temperature dependent study of the angular distribution of MDAD from ultrathin Co/Cu(001) films, using unpolarized Mg-K_α radiation. We have shown that in the experimental geometry used in the present investigation a strong deviation from the angular behavior of the dichroic asymmetry expected within an atomic description is observed. That deviation is related to crystallinity effects, which are found to be mainly governed by diffraction from forward scattering. This proves the diffraction picture in MDAD as introduced in Refs.[18,29,30], showing that such effects indeed play a crucial role in MDAD.

In particular for the 5 ML and 3 ML films the dichroic signal off the sample normal is dominated by diffraction. The diffraction effects are found to be reduced at 3 ML Co thickness, and much reduced at 1.5 ML, when only few atoms for forward scattering are available. The residual modulation at 2 ML and 1.5 ML must be related to the morphology of these films. A reduction of the diffraction contribution is observed in the 5 ML film at higher temperatures (300 K) with respect to the one measured at 100 K. This is explained with a loss of scattering coherence due to thermal vibrations of the solid atoms, which affects the photoelectron intensity and reduces the modulation in the angular distribution of the dichroic asymmetry (Debye-Waller effect).

A $(45 \pm 14)\%$ reduction of the atomic-like dichroism is observed along the sample normal when reducing the Co film thickness from 5 ML to 1.5 ML. This is discussed in connection with thermal effects near the Curie temperature of 1.5 ML, which decrease the magnetization in the 1.5 ML film. At 5 ML the atomic-like dichroism is almost unaffected by temperature variation from 300 K to 100 K. This is consistent with an unchanged magnetization of 5 ML at 100 K and 300 K due to the much higher Curie temperature.

The atomic-like dichroism in between the $2p_{3/2}$ and $2p_{1/2}$ lines is strongly structured showing that many body interaction effects play an important role in the shape of Co core level spectra.

Acknowledgement

We would like to thank A. Chassé and C. S. Fadley for many valuable discussions, and B. Zada for her expert technical support. One of us (M. S.) would like to thank the European Union for supporting his stay at the Max-Planck-Institut für Mikrostrukturphysik by a research fellowship (Human Capital and Mobility institutional grant).

References

[1] C. S. Fadley, D. A. Shirley, A. J. Freeman, P. S. Bagus, and J. V. Mallow, Phys. Rev. Lett., 23 (1969) 1397.

[2] C. S. Fadley, and D. A. Shirley, Phys. Rev. A, 2 (1970) 1109.

[3] J. L. Erskine, and E. A. Stern, Phys. Rev. B, 12 (1976) 5016.

[4] L. E. Klebanoff, D. G. Van Campen, and R. J. Pouliot, Phys. Rev. B, 49 (1994) 2047.

[5] D. G. Van Campen, and L. E. Klebanoff, Phys. Rev. B, 49 (1994) 2040.

[6] S. L. Qiu, R. G. Jordan, A. M. Begley, X. Wang, Y. Liu, and M. W. Ruckman, Phys. Rev. B, 46 (1992) 13 004.

[7] C. Carbone, and E. Kisker, Solid State Commun., 65 (1988) 1107.

[8] F. U. Hillebrecht, R. Jungblut, and E. Kisker, Phys. Rev. Lett., 65 (1990) 2450.

[9] C. Carbone, T. Rachel, R. Rochow, and W. Gudat, Solid State Commun., 77 (1991) 619.

[10] L. Baumgarten, C. M. Schneider, H. Petersen, F. Schäfers, and J. Kirschner, Phys. Rev. Lett., 65 (1990) 492.

[11] H. Ebert, L. Baumgarten, C. M. Schneider, and J. Kirschner, Phys. Rev. B, 44 (1991) 4406.

[12] C. M. Schneider, D. Venus, J. Kirschner, Phys. Rev. B, 45 (1992) 5041.

[13] D. Venus, L. Baumgarten, C. M. Schneider, C. Boeglin, and J. Kirschner, J. Phys. C, 5 (1993) 1239.

[14] Ch. Roth, F. U. Hillebrecht, H. B. Rose, and E. Kisker, Phys. Rev. Lett., 70 (1993) 3479.

[15] G. Rossi, F. Sirotti, N. A. Cherepkov, F. Combet Farnoux, and G. Panaccione, Solid State Commun., 90 (1994) 557.

[16] W. Kuch, M.-T. Lin, W. Steinhögl, C. M. Schneider, D. Venus, and J. Kirschner, Phys. Rev. B, 51 (1994) 609.

[17] M. Getzlaff, Ch. Ostertag, G. H. Fecher, N. A. Cherepkov, and G. Schönhense, Phys. Rev. Lett., 72 (1994) 3030.

[18] A. Fanelsa, R. Schellenberg, F. U. Hillebrecht, E. Kisker, J. G. Menchero, A. P. Kaduwela, C. S. Fadley, and M. A. Van Hove, Phys. Rev. B, 54 (1996) 17 962.

[19] C. M. Schneider, U. Pracht, W. Kuch, A. Chassé, and J. Kirschner, Phys. Rev. B, 54 (1996) R 15 618.

[20] G. Rossi, G. Panaccione, F. Sirotti, S. Lizzit, A. Baraldi, and G. Paolucci, Phys. Rev. B, 55 (1997) 11 488.

[21] D. Venus, Phys. Rev. B, 49 (1994) 8821.

[22] N. A. Cherepkov, Phys. Rev. B, 50 (1994) 13 813.

[23] N. A. Cherepkov, and V. V. Kuznetsov, J. Phys. B, 22 (1989) L405.

[24] U. Heinzmann, and G. Schönhense, in R. Feder (Ed.), Polarized Electrons in Surface Physics, World Scientific, Singapore, 1985.

[25] C. M. Schneider and J. Kirschner, Crit. Rev. Solid State Mater. Sci., 20 (1995) 179.

[26] G. Schönhense, Phys. Rev. Lett., 44 (1980) 640.

[27] B. T. Thole, and G. van der Laan, Phys. Rev. B, 49 (1994) 9613.

[28] N. A. Cherepkov, Sov. Phys. JETP, 38 (1974) 463.

[29] F. U. Hillebrecht, Ch. Roth, H. B. Rose, W. G. Park, E. Kisker, and N. A. Cherepkov, Phys. Rev. B, 53 (1996) 12 182.

[30] R. Schellenberg, E. Kisker, A. Fanelsa, F. U. Hillebrecht, J. G. Menchero, A. P. Kaduwela, C. S. Fadley, and M. A. Van Hove, Phys. Rev. B, 57 (1998) 14 310.

[31] R. Schellenberg, E. Kisker, M. Faust, A. Fanelsa, and F. U. Hillebrecht, Phys. Rev. B, 58 (1998) 81.

[32] C. S. Fadley, in R. Z. Bachrach (Ed.), Synchrotron Radiation Research: Advances in Surface Science, Plenum, New York, 1992.

[33] C. S. Fadley, Surf. Sci. Rep., 19 (1993) 231.

[34] C. S. Fadley, M. A. Van Hove, Z. Hussain, and A. P. Kaduwela, J. Electron Spectrosc. Relat. Phenom., 75 (1995) 273.

[35] A. P. Kaduwela, H. Xiao, S. Thevuthasan, C. S. Fadley, and M. A. Van Hove, Phys. Rev. B, 52 (1995) 14 927.

[36] J. R. Cerdá, P. L. de Andres, A. Cebollada, R. Miranda, E. Navas, P. Schuster, C. M. Schneider, and J. Kirschner, J. Phys.: Cond. Matt., 5 (1993) 2055.

[37] C. M. Schneider, A. K. Schmid, P. Schuster, H. P. Oepen, and J. Kirschner, in R. F. Farrow, M. Donath, B. Dieny, A. Fert, and B. Hermsmeier (Eds.), Structure and Magnetism in Low-Dimensional Systems, Plenum, New York, 1993.

[38] C. M. Schneider, P. Bressler, P. Schuster, J. Kirschner, J. J. de Miguel, R. Miranda, and S. Ferrer, Vacuum, 41 (1990) 503.

[39] C. M. Schneider, P. Bressler, P. Schuster, J. Kirschner, J. J. de Miguel, and R. Miranda, Phys. Lett., 64 (1990) 1059.

[40] B. Heinrich, J. F. Cochran, M. Kowalewski, J. Kirschner, Z. Celinski, A. S. Arrott, and K. Myrtle, Phys. Rev. B, 44 (1991) 9348.

[41] M. Kowalewski, C. M. Schneider, and B. Heinrich, Phys. Rev. B, 47 (1993) 8748.

[42] H. A. Wierenga, W. de Jong, M. W. J. Prins, T. Rasing, R. Vollmer, A. Kirilyuk, H. Schwabe, and J. Kirschner, Phys. Rev. Lett., 74 (1995) 1462.

[43] Q. Y. Jin, H. Regensburger, R. Vollmer, and J. Kirschner, Phys. Rev. Lett., 80 (1998) 4056.

[44] C. M. Schneider, Ph. D. Thesis, Free University Berlin, unpublished (1990), and references therein.

[45] C. M. Schneider, P. Bressler, P. Schuster, J. Kirschner, J. J. de Miguel, and R. Miranda, Phys. Rev. Lett., 64 (1990) 1059.

[46] A. Clarke, G. Jennings, R. F. Willis, P. J. Rous, and J. B. Pendry, Surf. Sci., 187 (1987) 327.

[47] B. Poserow, Q. Jang, and G. C. Wang, Surf. Sci., 388 (1997) 103.

[48] J. Fassbender, R. Allenspach, and U. Dürig, Surf. Sci., 383 (1997) L742.

[49] F. Nouvertné, U. May, M. Bamming, A. Rampe, U. Korte, G. Güntherodt, R. Pentcheva, and M. Scheffler, Phys. Rev. B, 60 (1999) 14 382.

[50] Xingyu Gao, Ph. D. Thesis, Martin-Luther-University Halle-Wittenberg, unpublished.

[51] S. Doniach, and M. Šunjić, J. Phys. C, 3 (1970) 285.

[52] P. Rennert and Yu Kucherenko, J. Electron Spectrosc. Relat. Phenom., 76 (1995) 157.

[53] Xingyu Gao, M. Salvietti, W. Kuch, C. M. Schneider, and J. Kirschner, Phys. Rev. B, 58 (1998) 15 426. .

[54] J. Kohlhepp, H. J. Elmers, S. Cordes, and U. Gradmann, Phys. Rev. B, 45 (1992) 12 287.

[55] A. K. See and L. E. Klebanoff, Phys. Rev. Lett., 74 (1995) 1454.

[56] A. K. See and L. E. Klebanoff, Phys. Rev. B, 51 (1995) 11 002.

[57] B. T. Thole and G. van der Laan, Phys. Rev. Lett., 67 (1991) 3306; Phys. Rev. B, 44 (1991) 12 424.

Fig. 1. Sketch of the experimental geometry showing the direction of the sample magnetization **M** along the [010] or [0$\overline{1}$0] crystallographic direction, the photon and photoelectron wavevectors (**q** and **k**, respectively), and the light electric field components. The angle between **q** and **k** is kept fixed at 45°. The rotation axis of the sample is along the direction of magnetization. Rotating the sample we vary the emission angle α between the surface normal **n** and the photoelectron wavevector **k**.

Fig. 2. (a) Co $2p$ intensity spectra collected in the experimental geometry indicated in Fig. 1, for magnetization positive (along [010], upward triangles) and negative (along [0$\overline{1}$0], downward triangles). The film is 5 ML Co/Cu(001), grown at room temperature. The sample temperature was 100 K, and the emission angle $\alpha = 0$. The energy scale is the binding energy relative to the Co $2p_{3/2}$ intensity peak, fixed as zero of the energy scale. The arrow marks the position of a correlation induced satellite. (b) Dichroic asymmetry calculated from the photoemission intensity curves of (a). The data points (circles) are shown base-line corrected, the solid line is the scaled template asymmetry spectrum. Features A and B indicate the "plus" and "minus" features of the Co $2p_{3/2}$ dichroism, respectively. Feature C marks the position of a correlation-induced satellite.

Fig. 3. Dichroic asymmetry curves after correction of the baseline (filled circles) for a 5 ML Co/Cu(001) film at the emission angles α indicated on the right hand side, measured at 100 K temperature. The solid lines are the template curves scaled with a constant parameter at each angle. The asymmetry scale is in percent, and is reported in the upper left side of the figure as reference. The curves are horizontally offset for clarity. The horizontal lines indicate zero asymmetry for each curve.

Fig. 4. As Fig. 3, but for a temperature of 300 K.

Fig. 5. (a) Angular distribution of the intensity of the Co $2p_{3/2}$ photoemission peak for 1.5 ML (solid circles), 2 ML (open squares), 3 ML (solid squares), and 5 ML Co films (open circles) at 100 K. For clarity the angular distribution of the 2 ML and 3 ML films have been shifted along the vertical axis by $2{\cdot}10^5$ and $2.5{\cdot}10^5$ counts, respectively. All data points have been acquired under identical experimental conditions. (b) Angular distribution of the Co $2p_{3/2}$ peak-to-peak asymmetry for 1.5 ML (solid circles), 2 ML (open squares), 3 ML (solid squares), and 5 ML Co films (open circles) at 100 K. The lines are for guiding the eye.

Fig. 6. (a) Angular distribution of the intensity of the Co $2p_{3/2}$ photoemission peak for 5 ML Co at 300 K (open circles) and 100 K (solid circles). The data points at 300 K have been collected with a 12.5% lower power of the x-ray source. (b) Angular distribution of the Co $2p_{3/2}$ peak-to-peak asymmetry for 5 ML Co at 300 K (open circles) and 100 K (solid circles). The lines are for guiding the eye.

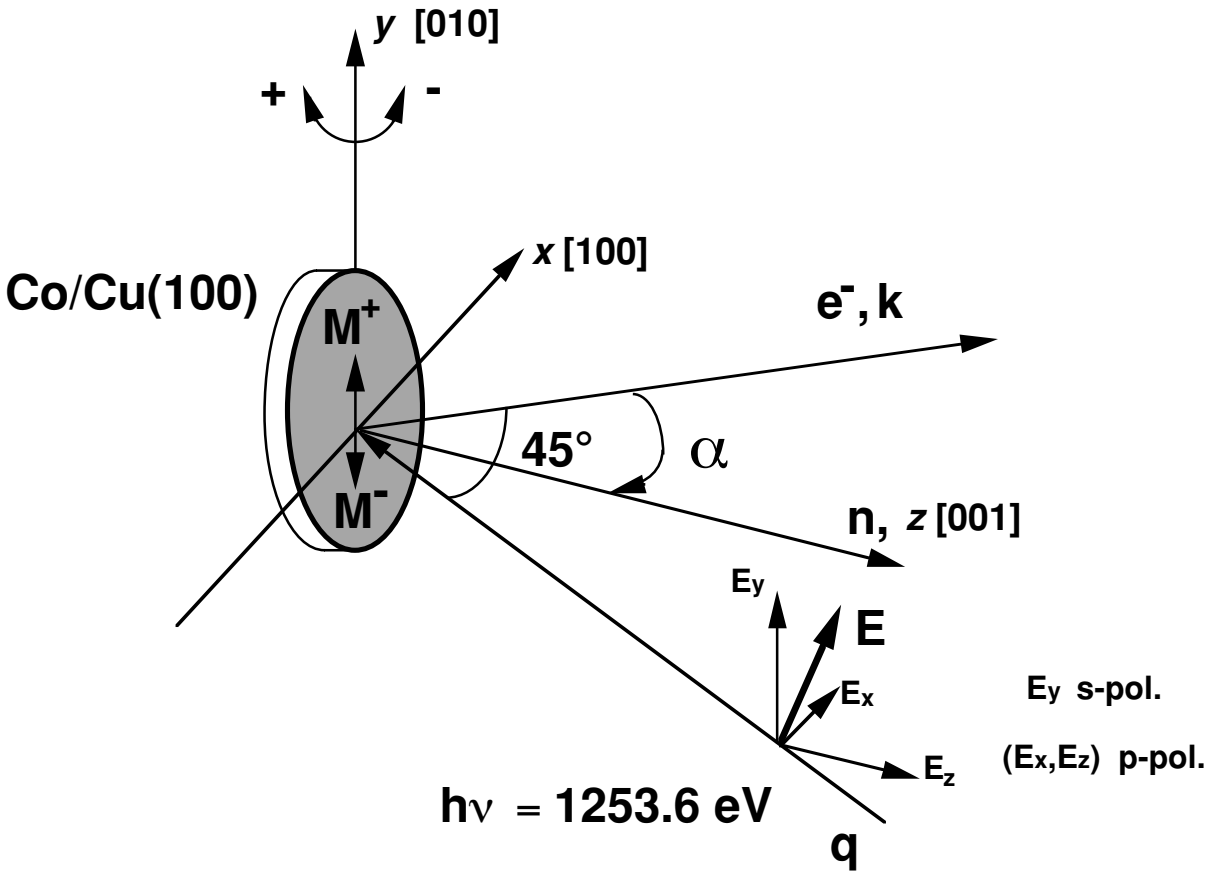
y [010]
+
-
x [100]
Co/Cu(100)
M+
M-
e-, k
45°
α
n, z [001]
Ey
E
Ex
Ez
Ey s-pol.
(Ex,Ez) p-pol.
hν = 1253.6 eV
q

Fig. 1

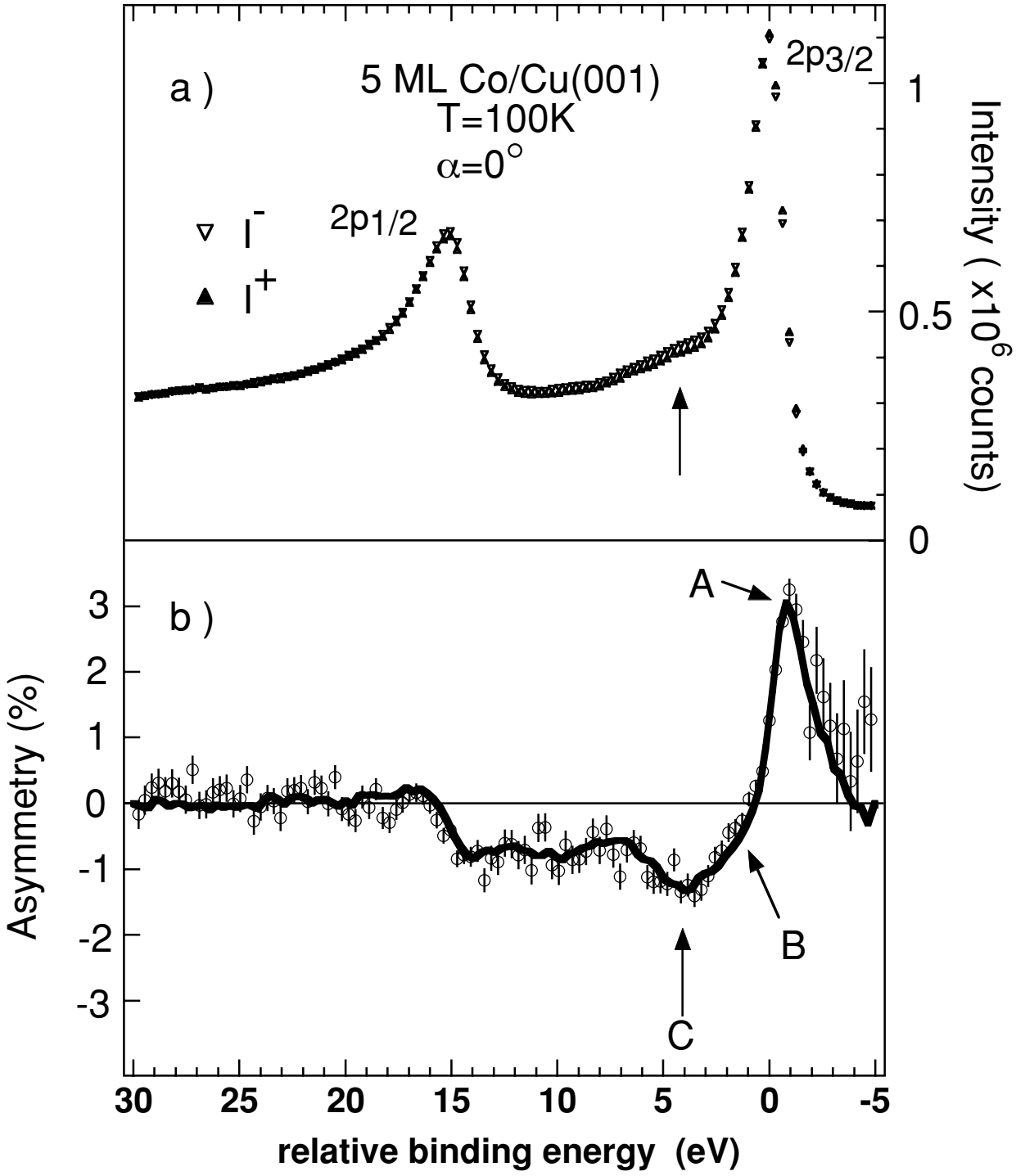
a)
5 ML Co/Cu(001)
T=100K
α=0°
2p3/2
2p1/2
I-
I+
Intensity (x10^6 counts)
1
0.5
0
b)
A
B
C
Asymmetry (%)
3
2
1
0
-1
-2
-3
30
25
20
15
10
5
0
-5
relative binding energy (eV)

Fig. 2

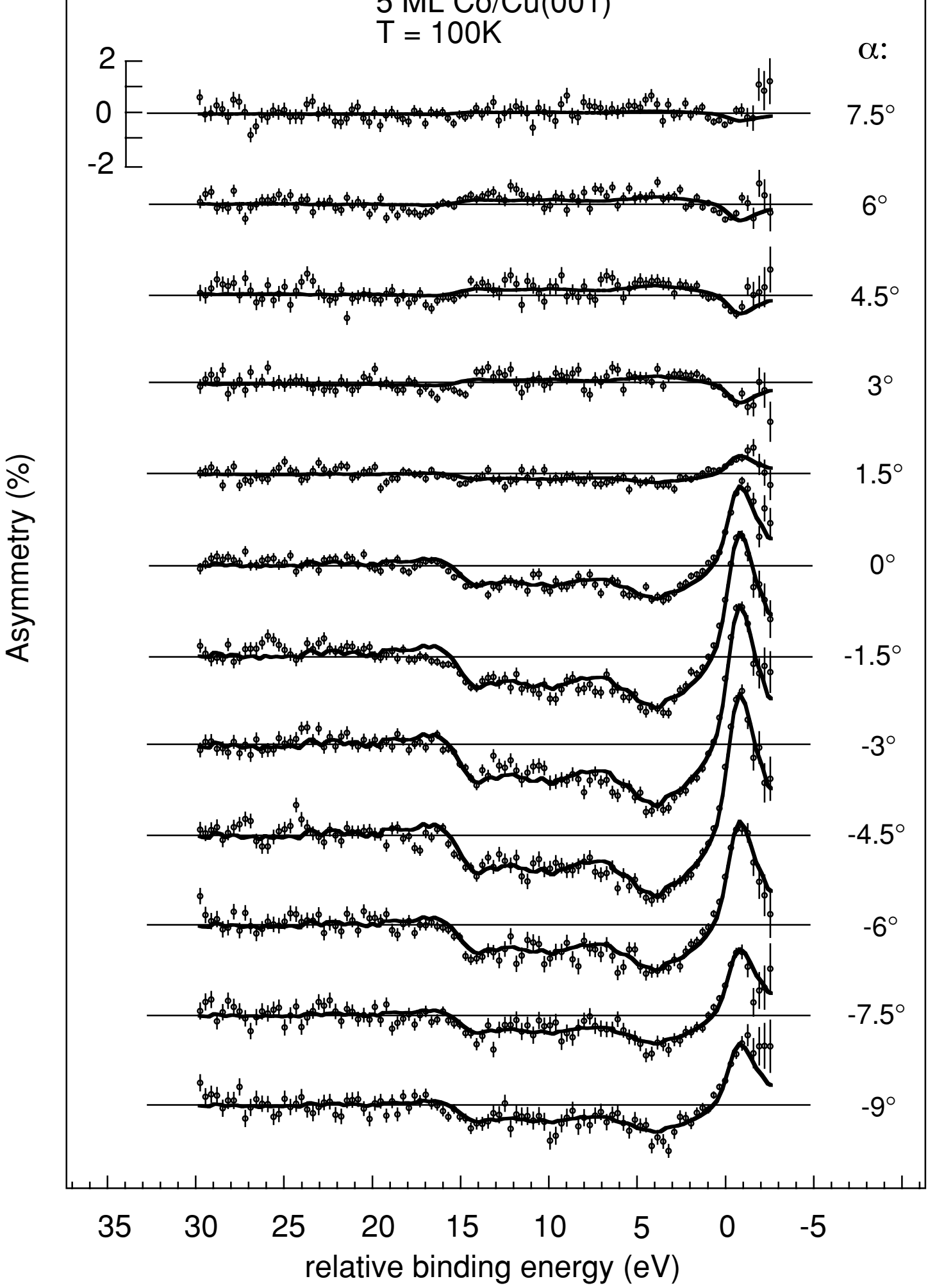
5 ML Co/Cu(001)
T = 100K
α:
7.5°
6°
4.5°
3°
1.5°
0°
-1.5°
-3°
-4.5°
-6°
-7.5°
-9°
2
0
-2
Asymmetry (%)
35
30
25
20
15
10
5
0
-5
relative binding energy (eV)

Fig. 3

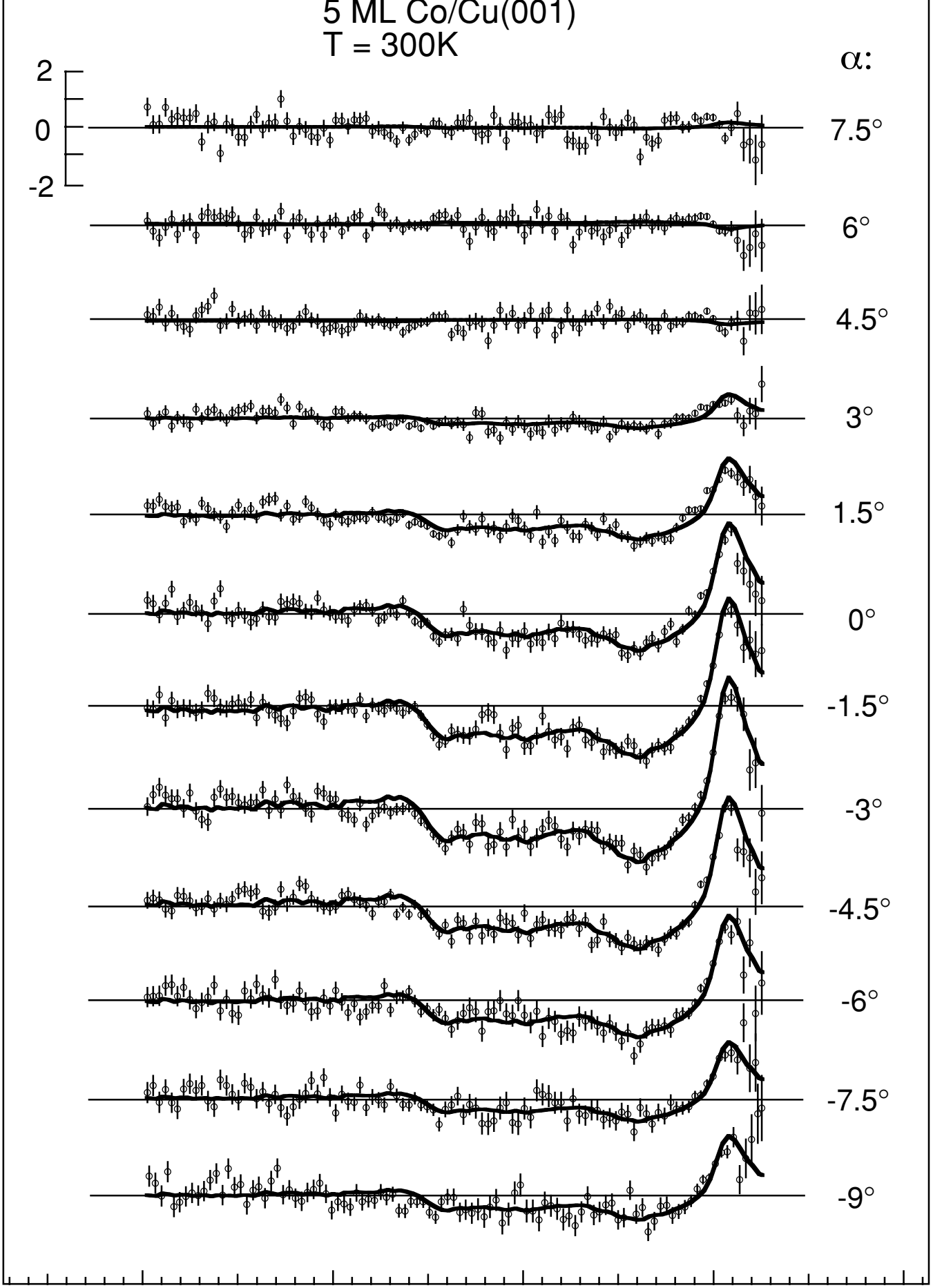
5 ML Co/Cu(001)
T = 300K
α:
2
0
-2
7.5°
6°
4.5°
3°
1.5°
0°
-1.5°
-3°
-4.5°
-6°
-7.5°
-9°
Asymmetry (%)
35
30
25
20
15
10
5
0
-5
relative binding energy (eV)

Fig. 4

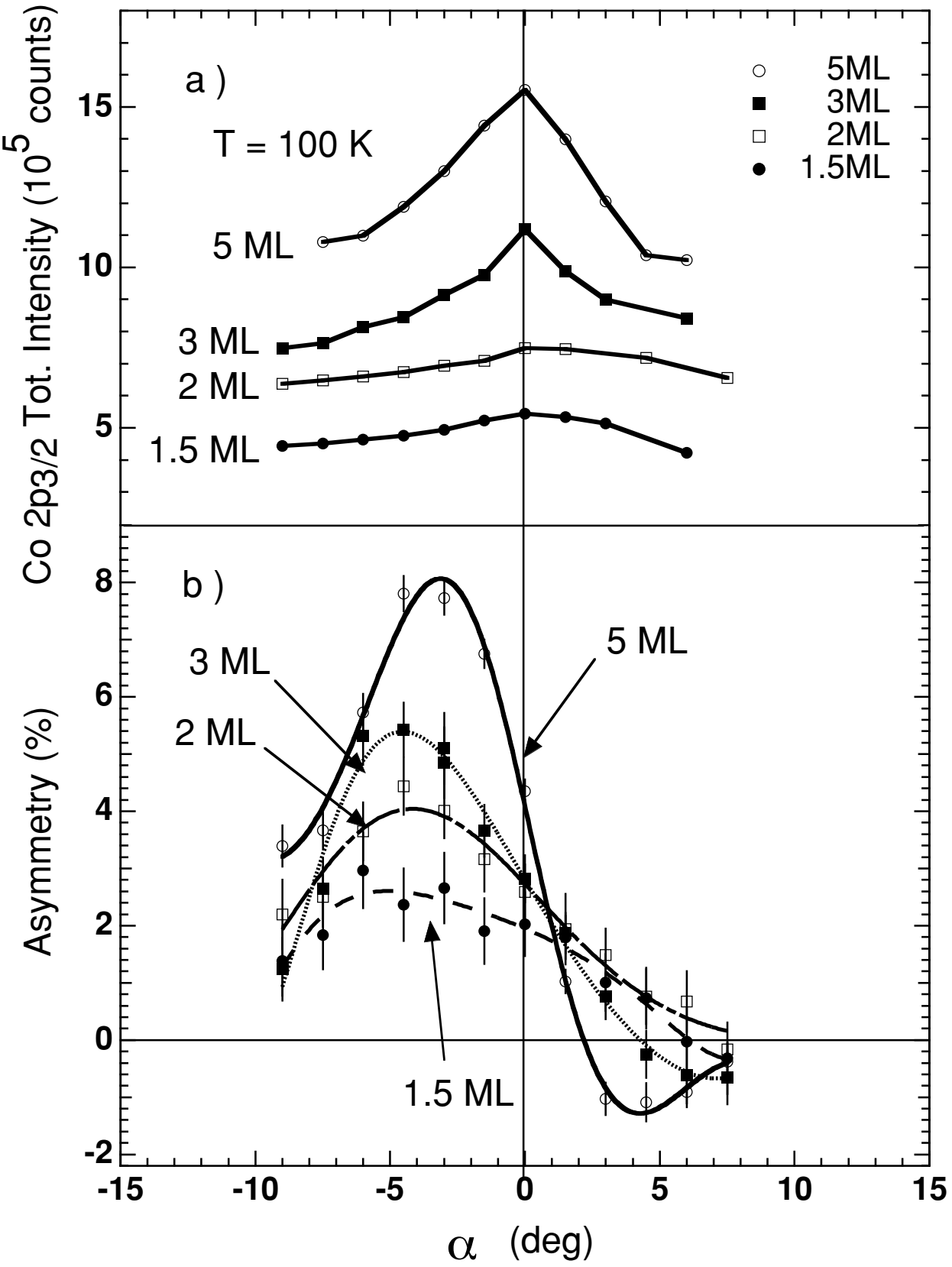
a)
T = 100 K
5 ML
3 ML
2 ML
1.5 ML
5ML
3ML
2ML
1.5ML
Co 2p3/2 Tot. Intensity (10^5 counts)
b)
3 ML
2 ML
5 ML
1.5 ML
Asymmetry (%)
α (deg)

Fig. 5

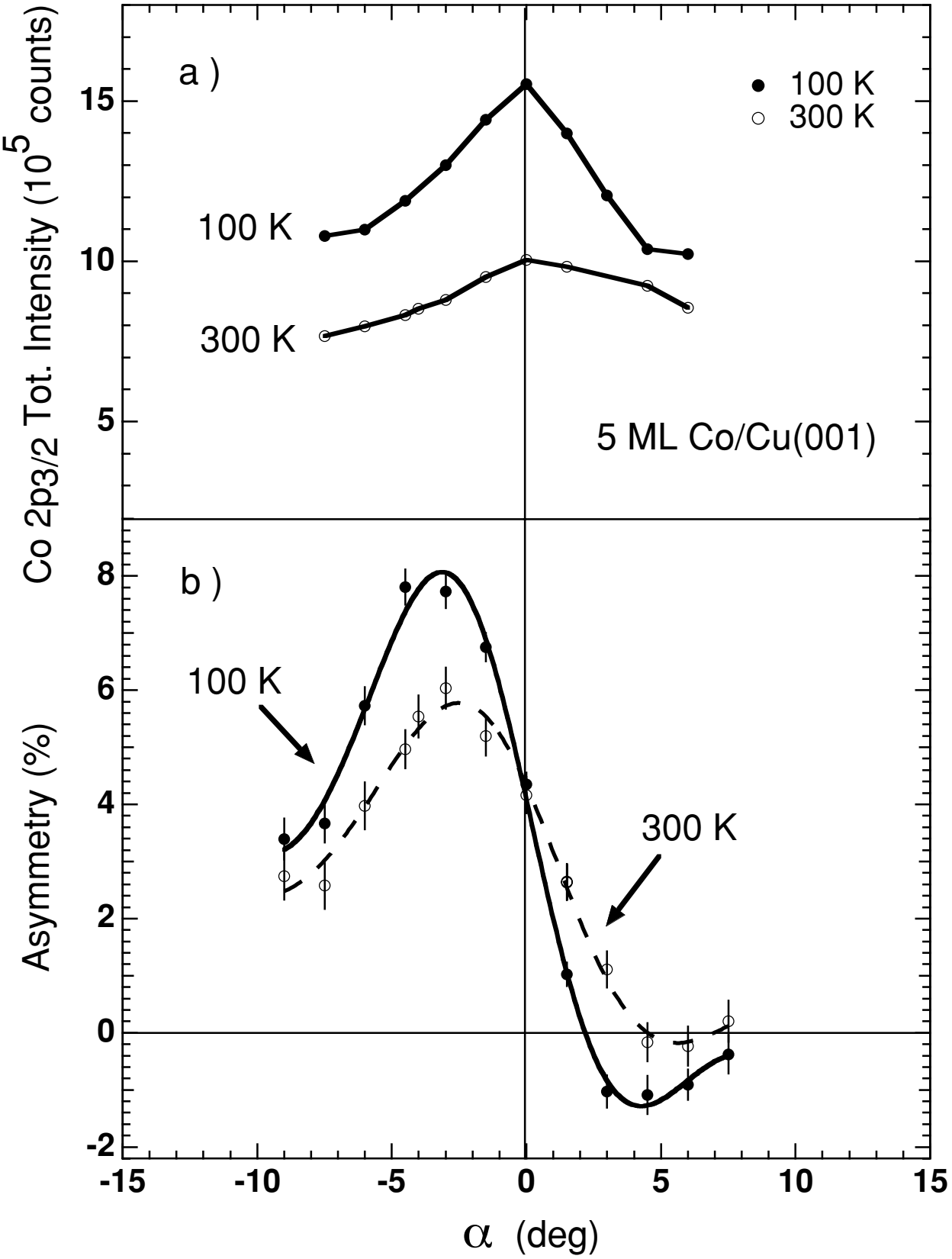
a)
100 K
300 K
100 K
300 K
5 ML Co/Cu(001)
Co 2p3/2 Tot. Intensity (10^5 counts)
b)
100 K
300 K
Asymmetry (%)
α (deg)

Fig. 6